Large-Signal Stability Improvement of DC-DC Converters in DC Microgrid

Gui, Yonghao; Han, Renke; Guerrero, Josep M.; Vasquez, Juan C.; Wei, Baoze; Kim, Wonhee

Published in:
I E E E Transactions on Energy Conversion

DOI (link to publication from Publisher):
10.1109/TEC.2021.3057130

Publication date:
2021

Document Version
Accepted author manuscript, peer reviewed version

Large-Signal Stability Improvement of DC-DC Converters in DC Microgrid

Yonghao Gui, *Senior Member, IEEE*, Renke Han, *Member, IEEE*, Josep M. Guerrero, *Fellow, IEEE*, Juan C. Vasquez, *Senior Member, IEEE*, Baoze Wei, *Member, IEEE*, and Wonhee Kim, *Member, IEEE*,

***Abstract*—In DC microgrids, constant power loads (CPLs) reduce the effective damping of the DC-DC converter and may induce destabilizing effects into the DC-DC converter. To overcome such problems regarding CPL and ensure large-signal stability of DC-DC converters in DC microgrids, some feedforward terms are added to *V-I* droop-based dual-loop controller for a DC-DC converter based on the large-signal model. It is proven that the feedforward terms can not only improve the transient response but also guarantee the exponential stability of the closed-loop system in the whole operating range in regards to a large-signal manner, which is verified by using a singular perturbation model. Moreover, a disturbance observer is designed to estimate the output current, thereby enabling the removal of the current measurement sensor. The proposed technique can be easily plugged into a pre-defined *V-I* droop-based dual-loop controller without an additional sensor being required. Ultimately, both simulation and experimental tests verify the effectiveness of the proposed method.**

***Index Terms*—DC–DC converter, DC microgrid, constant power load, exponentially stable, disturbance observer.**

I. Introduction

WITH the increased penetration of renewable energy resources (RESs) in electrical systems, control of power converters has been extensively discussed to increase the performance and reliability of the electrical system [1]–[3]. The concept of microgrid is an effective method for power generation and distribution with the integration of RES [4]. DC microgrids are considered to be more attractive for numerous applications due to their several advantages, such as higher efficiency, more natural interface to many types of RES and energy storage system, and better compliance with consumer electronics [5].

In DC microgrids, constant power loads (CPLs) reduce the effective damping of the DC-DC converter and may induce destabilizing effects into the DC-DC converter because CPLs exhibit nonlinear dynamics and negative incremental impedance [6]–[8]. Various literatures analyzed the stability for DC microgrids with CPLs. The stability around a fixed equilibrium point have been studied based on the normal operating conditions of the CPLs considering single converter [9]–[11] or multiple converters [12]–[16]. One of the main challenges will be the nonlinearity addressed by the CPLs [7]. As a consequent, CPLs present a significant challenge for system operation and control [17].

To resolve such CPL problems in DC-DC converters, various control strategies have been designed and analyzed. A negative input compensator was proposed to stabilize a brushless DC motor drive by modifying its input impedance [18]. The amplitude death methods were applied to overcome the stabilization problems of CPLs [19]. One of the simple and effective methods to overcome this problem was to employ a passive damping strategy, which adds a necessary capacitor or resistor [20] or design LC filters [21]. However, these methods require additional cost and have physical constraints. Another strategy is to employ active damping methods, such as virtual resistor [22], virtual capacitor [23], and virtual impedance [24], which overcome the CPL problems by emulating the passive elements through the modification of control loops. However, these active damping methods can deteriorate the load performance because they increase CPL damping. An active damping control method to emulate the virtual resistance of a source DC-DC buck converter that supply power to the paralleled CPLs with their input filter was presented in [25]. However, the bandwidth of the closed-loop system is changed to affect the system's dynamic response. In [26], an inertia and damping controller was proposed to improve voltage quality. However, all these methods were designed based on a small signal model. Although various linear control techniques can be easily applied into the small-signal model for control or analysis, the stability near the operating point can be guaranteed. In addition, it is not easy to guarantee a uniform and satisfactory control performance over the entire operating range. If a large disturbance occurs, then these linear control methods may become ineffective and the system may become unstable because of the CPL [27], [28].

To overcome such problems, several nonlinear control strategies have been designed for DC-DC converters based on the large signal model. In [29], a model predictive control (MPC) method was proposed for boost converters feeding a CPL; however, its implementation may be difficult due to the online computational burden of MPC. A state feedback linearization approach was proposed for a DC-DC buck converter loaded with a CPL to improve its transient per-

This research was supported by Energy Cloud R&D Program through the National Research Foundation of Korea (NRF) funded by the Ministry of Science, ICT (NRF-2019M3F2A1073313); This work was supported by VILLUM FONDEN under the VILLUM Investigator Grant (no. 25920): Center for Research on Microgrids (CROM); www.crom.et.aau.dk. (*Corresponding Author: Wonhee Kim*).

Y. Gui is with the Department of Electronic Systems, Aalborg University, 9220 Aalborg, Denmark (e-mail: yg@es.aau.dk).

R. Han is with the Department of Engineering Science, University of Oxford, OX1 3PJ, Oxford, UK (e-mail: renke.han@eng.ox.ac.uk).

J. M. Guerrero, J. C. Vasquez, and B. Wei are with the Department of Energy Technology, Aalborg University, 9220 Aalborg, Denmark (e-mail: joz@et.aau.dk; juq@et.aau.dk; bao@et.aau.dk).

W. Kim is with the School of Energy Systems Engineering, Chung-Ang University, Seoul 06974, South Korea (e-mail: whkim79@cau.ac.kr).

formance [30]. However, the feedback linearization approach is sensitive to noise from the output channels. To overcome this problem, a sliding-mode duty cycle ratio controller was proposed to stabilize the DC bus voltage in an application of the medium voltage DC shipboard power system [31]. In addition, a second-order sliding-mode control (SMC) method was developed to address the regulation problem of a DC-DC buck power converter [32]. The SMC method is insensitive to match uncertainties and achieving a fast response. However, it may present variable frequency switching and chattering problems. Considering the passivity of physical systems, a complementary proportional-integral controller based on the adaptive interconnection and damping assignment passivity-based control technique was designed for a DC-DC boost converter [33]. It presents the advantages of simple implementation and robustness; however, it may be associated with sluggish transient response during the variation of the operating point. To compensate for the uncertainties and/or the disturbance, the disturbance observer (DOB) based methods were proposed [34]. In [35], a robust output feedback controller based on a nonlinear DOB was proposed for DC-DC buck converters to handle the components' uncertainties. However, the authors of that study do not appear to consider the CPL problem. Recently, a backstepping controller was proposed to address the CPL problem. Xu et al. proposed an adaptive backstepping and nonlinear DOB control strategy to solve the stabilization problem of DC-DC boost converters feeding CPL [27]. Those methods improve the performance with the consideration of the nonlinear properties.

Our motivation is to design a simple yet robust control method in order to improve not only the transient response but also the stability and performance in the whole operating range. It is shown that the destabilizing effects of the CPL can be indirectly rejected by using the output current when using the V-I droop-based dual-loop controller. Consequently, a modified V-I droop-based dual-loop controller is designed to guarantee system stability under the effect of the CPL based on the large-signal model, which can be guaranteed the large-signal stability of DC-DC converters in DC microgrids. Although the feedforward terms can improve the transient response [36], in this paper, it also can guarantee the exponential stability of the closed-loop system in the whole operating range in regards of large signal manner even there exist constant power loads in DC microgrids. In addition, a DOB is designed to estimate the output current, which can reduce the cost of measurement sensor. The exponential stability of the closed-loop system is verified in the whole operating range by using a singular perturbation model because the DC-DC converter comprises an inner fast current loop and an outer slow voltage loop. It should be noted that although the feedforward controller for DC-DC converters has been designed [26], [37], [38], this paper firstly proves the exponential stability based on the large-signal model. The simulation results show that the proposed method solves the CPL problem and improves transient response. Finally, the experimental tests are conducted using the 2.2 kW DC-DC converter to verify its effectiveness. Both simulation and experimental results match the theoretical expectations closely. The main contribution are

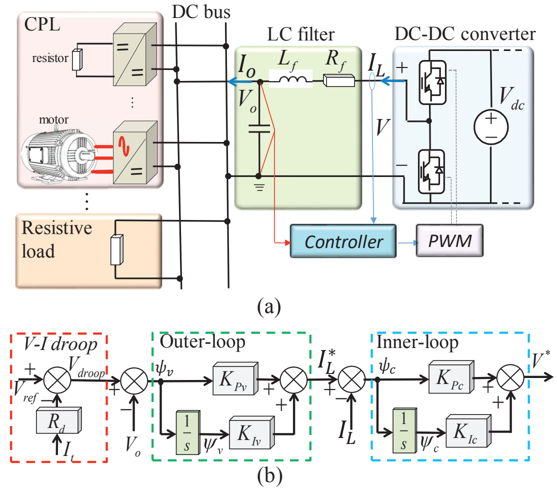

Fig. 1. (a) Converter in the DC microgrid. (b) Block diagram of V-I droop-based dual-loop control.

summarized as follows:

- Simple implementation: The proposed technique can be easily plugged into a pre-defined V-I droop-based dual-loop controller without the additional sensor.
- Stability and Robustness: The exponential stability of the closed-loop system is guaranteed by the proposed method under the constant power loads and is mathematically proven in a large-signal manner by using the singular perturbation theory.

II. Control DC-DC Converter in DC Microgrids

In this section, we introduce a DC voltage-controlled voltage source converter, which is controlled by using a V-I droop controller to regulate the voltage. The DC-DC converter supports the resistor load and CPL, as shown in Fig. 1(a). Further, it is shown that the CPL affects the system stability as well.

A. Converter model

In this study, the buck-type topology is used; thus, the dynamic model with an LC filter can be presented as follows:

$$\begin{aligned} \dot{I}_L &= \frac{1}{L_f}V^* - \frac{R_f}{L_f}I_L - \frac{1}{L_f}V_o \\ \dot{V}_o &= \frac{1}{C_f}I_L - \frac{1}{C_f}I_o, \end{aligned} \tag{1}$$

where I_L is the filter current, V^* is the converter voltage input, L_f is the filter inductor, R_f is the equivalent resistance of the inductor, C_f is the filter capacitor, and I_o is the output current. It should be noted that V^* is the control input of the system.

B. V-I droop-based dual-loop controller

In this study, we consider a V-I droop-based dual-loop controller for the DC-DC converter, where the V-I droop is used for current sharing in DC microgrids [39]. The V-I droop-based dual-loop controller can be expressed as

$$V_{droop} = V_{ref} - R_d I_L, \tag{2}$$

where V_{droop} is output of the droop control, V_{ref} is the voltage reference, and R_d is the droop coefficient. Further, the dual-control loop is generally designed as follows:

$$\dot{\psi}_v = V_{droop} - V_o, \tag{3a}$$

$$I_L^* = K_{Iv}\psi_v + K_{Pv}(V_{droop} - V_o), \tag{3b}$$

$$\dot{\psi}_c = I_L^* - I_L, \tag{3c}$$

$$V^* = K_{Ic}\psi_c + K_{Pc}(I_L^* - I_L), \tag{3d}$$

where K_{Iv}, K_{Pv}, K_{Ic}, and K_{Pc} are the positive controller gains. ψ_v and ψ_c are the auxiliary state variables defined for the PI controllers of the outer and inner loops, respectively. The control block diagram can be seen in Fig. 1(b). It should be noted that the V-I droop-based dual-loop controller consists of two parts. The V-I droop controller as given in (2), which is used to generate the voltage reference for dual-loop controller (also achieve roughly current sharing when applied for multi-converter system). The dual-loop controller is a cascade structure consisting of two conventional PI controllers, in which, the voltage controller is the outer loop PI controller to generate the reference of the inner loop (current loop) and the current loop is the inner loop PI controller to generate the control signal for PWM generator. Essentially, the outer loop is to guarantee the voltage tracking the reference, and the inner loop is to limit the current response.

By combining (2) with (3), the completed voltage-controlled voltage source converter model is shown as

$$\dot{X}_{VSC} = A_{VSC}X_{VSC} + \begin{bmatrix} B_{VSC_1} & B_{VSC_2} \end{bmatrix} U, \tag{4}$$

where

$$\begin{aligned}
&X_{VSC} = \begin{bmatrix} V_o & I_L & \psi_v & \psi_c \end{bmatrix}^T, U = \begin{bmatrix} V_{ref} & I_o \end{bmatrix}^T.\\
&A_{VSCi} = \begin{bmatrix} 0 & \frac{1}{C_f} & 0 & 0 \\ a & b & \frac{K_{Pc}K_{Iv}}{L_f} & \frac{K_{Ic}}{L_f} \\ -1 & -R_d & 0 & 0 \\ -K_{Pv} & -K_{Pv}R_d - 1 & K_{Iv} & 0 \end{bmatrix},\\
&a = -\frac{K_{Pc}K_{Pv}+1}{L_f}, \quad b = -\frac{K_{Pc}K_{Pv}R_d + K_{Pc} + R_f}{L_f},\\
&B_{VSC_1} = \begin{bmatrix} 0 & \frac{K_{Pc}K_{Pv}}{L_f} & 1 & K_{Pv} \end{bmatrix}^T,\\
&B_{VSC_2} = \begin{bmatrix} -\frac{1}{C_f} & 0 & 0 & 0 \end{bmatrix}^T.
\end{aligned} \tag{5}$$

C. Load model

First, the output current, I_o, consists of the currents of the resistive load and CPL.

$$I_o = I_{o\_R} + I_{o\_CPL}(v) \tag{6}$$

where I_{o_R} and $I_{o\_CPL}(v)$ represent the output current for the resistive load and the CPL, respectively. The resistive load is considered as

$$I_{o\_R} = G_{L\_R}V_o, \tag{7}$$

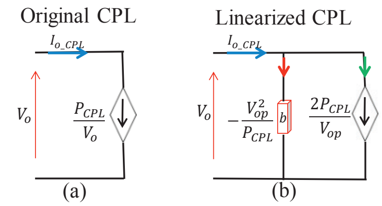

Fig. 2. Equivalent constant power load model..

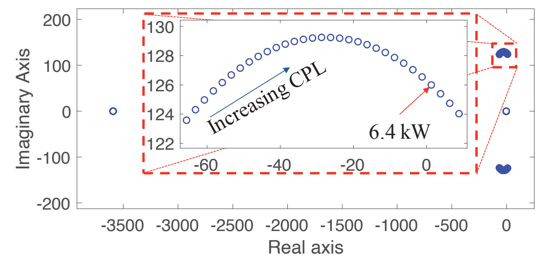

Fig. 3. Eigenvalues of the system when changing CPL from 1 to 7 kW.

where G_{L_R} represents the conductance of the resistive load. An ideal CPL model is nonlinear; thus, it is a common practice to linearize it in a voltage operating point, V_{op}, which is expressed as follows:

$$I_{o\_CPL}(v) \approx \underbrace{I_{CPL}}_{a} + \underbrace{\left(-P_{CPL}/V_{op}^2\right)v}_{b}, \tag{8}$$

where P_{CPL} is the constant power and $I_{CPL} = 2P_{CPL}/V_{op}$ is the equivalent constant current source.

In (8), part (a) is similar to a constant current load, which leads to oscillatory behavior. Part (b) is the negative impedance part, which can undermine the stability of the system. Each CPL is connected to the converter through a transmission line, as depicted in the equivalent model shown in Fig. 2. It should be noted that $v = V_o$ in (8) and V_{op} is an operating point value (steady-state value), which is required to obtain the model as shown in Fig. 2 Based on the above model, the instability phenomenon in terms of CPL can be derived [40]. With the parameters listed in Tables I and II, the eigenvalues of the system when changing CPL from 1 to 7 kW was shown in Fig. 3. This result was obtained for steady-state response of a linearization model around the given operating point when using the V-I droop-based dual-loop controller. One pair of poles of the closed-loop system goes across the imaginary axis to the right half plane when the CPL is changed to approximately 6.4 kW, as shown in Fig. 3, which means that the closed-loop system becomes unstable. Consequently, the previous V-I droop-based dual-loop controller has limitations in control performance. Furthermore, I_o in (5), which may make the system become unstable, should be compensated by the controller. This will be studied in the next section.

III. Controller Design

In this section, we design a controller to reject I_o in DC microgrids. Moreover, to avoid the addition of a sensor, we design a DOB to estimate I_o. Finally, the stability of the closed-loop system is mathematically proven.

A. Feedforward method

To compensate for I_o, I_L^* in (3b) is changed to the following expression:

$$I_L^* = K_{Iv}\psi_V + K_{Pv}(V_{droop} - V_o) \underbrace{+I_o}_{\text{Feedforward}} . \tag{9}$$

The term I_o is a feedforward term, which could be either obtained by a sensor or calculated by a DOB. To improve the control performance, the additional terms are included in V (3d) as

$$V^* = K_{Ic}\psi_c + K_{Pc}(I_L^* - I_L) \underbrace{+R_f I_L + V_o}_{\text{additional feedforward}} . \tag{10}$$

We define the tracking errors as

$$\begin{aligned} \psi_v &= \int_0^t e_v(\tau)d\tau, \qquad e_v = V_{droop} - V_o \\ \psi_c &= \int_0^t e_c(\tau)d\tau, \qquad e_c = I_L^* - I_L. \end{aligned} \tag{11}$$

Further, the tracking error dynamics are as follows:

$$\begin{aligned} \dot{\psi}_v &= e_v, \qquad \dot{e}_v = \dot{V}_{droop} - \frac{1}{C_f}I_L + \frac{1}{C_f}I_o \\ \dot{\psi}_c &= e_c, \qquad \dot{e}_c = \dot{I}_L^* - \frac{1}{L_f}(K_{Ic}\psi_c + K_{Pc}e_c). \end{aligned} \tag{12}$$

B. Disturbance observer

Assumption 1: The disturbance $I_o(t)$ in system (1) satisfies the two conditions as follows:

- The upper bound d^* of $|I_o|$ for all t exists such that
$$d^* = \sup|I_o(t)|, \tag{13}$$
- $\dot{I}_o$ converges to zero such as
$$\lim_{t\to\infty} \dot{I}_o(t) = 0. \tag{14}$$

It should be noted that Assumption 1 is always acceptable in DC microgrid [37], [41]. The DOB for estimating I_o is designed by

$$\begin{aligned} \dot{z} &= -\frac{\ell}{C_f}z + \frac{\ell^2}{C_f}V_o + \frac{\ell}{C_f}I_L \\ \hat{I}_o &= z - \ell V_o, \end{aligned} \tag{15}$$

where z is the intermediate state of an observer, and ℓ is the observer gain. We define $e_d = I_o - \hat{I}_o$. Further,

$$\begin{aligned} \dot{e}_d &= \dot{I}_o - \dot{\hat{I}}_o \\ &= -\frac{\ell}{C_f}e_d + \dot{I}_o. \end{aligned} \tag{16}$$

If we select $\ell > 0$ to guarantee the system stability, then e_d exponentially converges to zero as per (14). Fig. 4 shows the control block diagram of the proposed method and the DOB plugged-in the existing the V-I droop-based dual-loop controller . It can be seen that the bottom part is the V-I droop-based dual-loop controller including additional feedforward terms in (10), which is indicated by a green-dashed box in Fig. 4. Then, the feedforward term, I_o, can be added into the generation of I_L^* in (9) in order to overcome the CPL problem in DC microgrid. I_o can be replaced by $\hat{I}_o$, which is estimated by the DOB (15) in a blue-dashed box of Fig. 4..

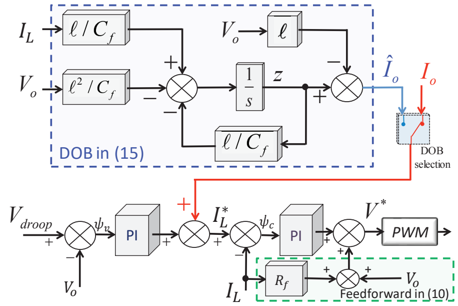

Fig. 4. Control block diagram of the proposed method.

C. Singular perturbation model

A general standard full singular perturbed system [42], [43] is in the form of

$$\begin{aligned} \dot{x} &= f(t,x,z,\varepsilon) \\ \varepsilon\dot{z} &= g(t,x,z,\varepsilon), \end{aligned} \tag{17}$$

where f and g are continuously differentiable, $x \in \mathbb{R}^n$ is the state of the slow subsystem, $z \in \mathbb{R}^m$ is the state of the fast subsystem, and ε is a small positive parameter. We use $x(t,\varepsilon)$ and $z(t,\varepsilon)$ to denote the solution of the full singular perturbation problem. The main objective behind using a singular perturbation method is to divide the dynamics of the system into two separate time-scales, so that the resulting design problem is easier to solve than the design problem of a full singularly perturbed system [42], [43]. From Theorem 11.4 discussed in [43], if the boundary-layer model and the reduced-order system are exponentially stable, then there exists a positive constant ε^* such that for $0 < \varepsilon < \varepsilon^*$, the origin of the system (17) is exponentially stable.

Practically, in all well-designed converters, L_f can play the role of the parameter ε [43] so that the converter model can be interpreted as the singular perturbed model. In the estimation error dynamics (III-C), ℓ can be designed such that $\frac{\ell}{C_f} = \frac{1}{\varepsilon}$. Further, the tracking error dynamics (12) and estimation error dynamics can be rewritten in the form of a singular perturbation model as follows

$$\begin{aligned} \dot{\psi}_v &= f_1(t,e_1,e_c,e_d) = e_v \\ \dot{e}_v &= f_2(t,e_1,e_c,e_d) = \dot{V}_{droop} - \frac{1}{C_f}I_L + \frac{1}{C_f}I_o \\ \dot{\psi}_c &= f_3(t,e_1,e_c,e_d) = e_c \\ \varepsilon\dot{e}_c &= g_1(t,e_1,e_c,e_d,\varepsilon) = \varepsilon\dot{I}_L^* - (K_{Ic}\psi_c + K_{Pc}e_c) \\ \varepsilon\dot{e}_d &= g_2(t,e_1,e_c,e_d,\varepsilon) = -e_d, \end{aligned} \tag{18}$$

where $e_1 = [\psi_v,\ e_v,\ \psi_c]^T$.We define $\bar{e}_c$ as

$$\bar{e}_c = -\frac{K_{Ic}}{K_{Pc}}\psi_c = h(\psi_c). \tag{19}$$

Let us define y_e as

$$y_e = e_c - h(\psi_c). \tag{20}$$

Differentiating and multiplying ε on both sides of (20) results in

$$\varepsilon \dot{y}_e = \varepsilon \dot{e}_c - \varepsilon \dot{h}(\psi_c). \tag{21}$$

With a new time variable $\frac{d\tau}{dt} = \frac{1}{\varepsilon}$ and $\varepsilon = 0$, the boundary-layer system for (19) is obtained as

$$\begin{aligned} \frac{dy_e}{d\tau} &= g_1(t, e_1, y_e + h, e_d, 0) \\ &= -K_{Pc} y_e \\ \frac{de_d}{d\tau} &= g_2(t, e_1, y_e + h, e_d, 0) \\ &= -e_d. \end{aligned} \tag{22}$$

If $K_{Pc} > 0$, the origin of the boundary-layer system (22) is exponentially stable. Furthermore, the region of attraction of the fast manifold covers the entire domain. From Theorem 3.1 discussed in [42], the eigenvalues of the fast dynamics can be approximated as

$$\begin{aligned} \lambda_c &= \frac{-K_{Pc} + O(\varepsilon)}{\varepsilon} \\ \lambda_d &= \frac{-1 + O(\varepsilon)}{\varepsilon}. \end{aligned} \tag{23}$$

Therefore, $L_f = \varepsilon$ is smaller, i.e. the fast dynamics play a small role in the transient response. The quasi-steady-states are

$$\begin{aligned} e_c &= \bar{e}_c = -\frac{K_{Ic}}{K_{Pc}} \psi_c \\ e_d &= 0. \end{aligned} \tag{24}$$

V_{ref} is a constant value; thus, we assume that $\dot{V}_{droop} = 0$ is in the quasi-steady-states. Moreover, $\dot{I}_L \approx 0$ is in the outer loop, because the current dynamics with the inner loop is faster than the voltage dynamics [39]. Thus, the reduced-order model dynamics are given as

$$\begin{aligned} \dot{\psi}_v &= f_1(t, e_1, \bar{e}_c, 0) = e_v \\ \dot{e}_v &= f_2(t, e_1, \bar{e}_c, 0) = -K_{Iv} \psi_V - K_{Pv} e_v \\ \dot{\psi}_c &= f_3(t, e_1, \bar{e}_c, 0) = -\frac{K_{Ic}}{K_{Pc}} \psi_c. \end{aligned} \tag{25}$$

If K_{Ic}, K_{Pc}, K_{Iv} and K_{Pv} are chosen such that $\frac{K_{Ic}}{K_{Pc}} > 0$ and the polynomial $s^2 + K_{Pc}s + K_{Ic} = 0$ and $s^2 + K_{Pv}s + K_{Iv} = 0$ are Hurwitz, then, the origin of the reduced-order model dynamics (25) is exponentially stable. Finally, we conclude that the origins of the boundary-layer and reduced-order models are exponentially stable. Therefore, using Theorem 11.4 discussed in [43], there exists a positive constant ε^* such that for $0 < \varepsilon < \varepsilon^*$ the tracking error e exponentially converges to zero.

Remark 1: The proposed method guarantees the exponential stability of the zero equilibrium point of the closed loop (19); thus, the proposed method guarantees robustness against the parameter uncertainties if they are in the form of vanishing perturbation terms. However, they are in the form of nonvanishing perturbation terms, the proposed method guarantees only boundedness of the tracking error and estimation error. The detailed robustness analysis is another problem and is beyond the scope of this study; however, it is discussed in [44], [45].

Remark 2: Although the feedforward controller has been designed [26], [37], this paper firstly proves the exponential stability based on the large-signal model.

Remark 3: The convergence of the errors to the zero in (19) is guaranteed with the assumption that $\lim_{t\to\infty} \dot{I}_o(t) = 0$. If $\lim_{t\to\infty} \dot{I}_o(t) \neq 0$, the boundedness of the disturbance estimation error is guaranteed as $|e_d(t)| \leq e^{-\frac{\ell}{C_f}t} \cdot e_d(0) + \frac{1}{l} \sup_t \dot{I}_o(t)$. In this case, only boundedness of the errors is guaranteed.

TABLE I
SYSTEM PARAMETERS USED IN THE SIMULATION AND EXPERIMENT

Parameter	Symbol	Value	Unit
DC source	V_{dc}	200	V
Nominal bus voltage	V_o^*	100	V
Filter inductance	L_f	1.8	mH
Filter resistance	R_f	0.1	Ω
Filter capacitor	C_f	2200	μF
Switching frequency	f_s	10	kHz
Sampling time	T_s	0.1	ms
CPL parameter			
Output DC voltage	$V_{dc,cpl}$	50	V
Input filter inductance	$L_{cpl,f}$	1	mH
Input filter resistance	$R_{cpl,f}$	0.1	Ω
Input filter capacitor	$C_{cpl,f}$	2200	μF
Output filter inductance	$L_{cpl,o}$	18	mH
Output filter resistance	$R_{cpl,o}$	0.1	Ω
Output filter capacitor	$C_{cpl,o}$	2200	μF
Switching frequency	f_{cpl}	10	kHz
Sampling time	T_{cpl}	0.1	ms

TABLE II
CONTROLLER GAINS USED IN THE SIMULATION.

Symbol	K_{Pv}	K_{Iv}	K_{Pc}	K_{Ic}	ℓ	R_d
Value	0.5	100	6	20	50	0.26

IV. SIMULATIONS

To validate the proposed current modulation method, MATLAB/Simulink, Simscape Power Systems is used. The system parameters are listed in Table I. In the simulations, we use the conventional *V-I* droop-based dual-loop controller (3) described in Section II-B to compare the performance of the proposed method. The proposed method involves two aspects; one is the output current measurement and the other is based on the designed DOB in (15). It should be noted that, the same controller gains are used for the *V-I* droop and dual-loop in both conventional and proposed methods. In addition, a DC-DC converter is used to emulate a CPL, where the output voltage of the CPL is controlled at a constant value (50 V).

A. Transient Response

Fig. 5 shows the time response of the output voltage and current of the DC-DC converter when the CPL is increased in the microgrid. The red-dotted, green-solid, and blue-dashed lines represent the conventional *V-I* droop-based dual-loop controller, the proposed current modulation method with the

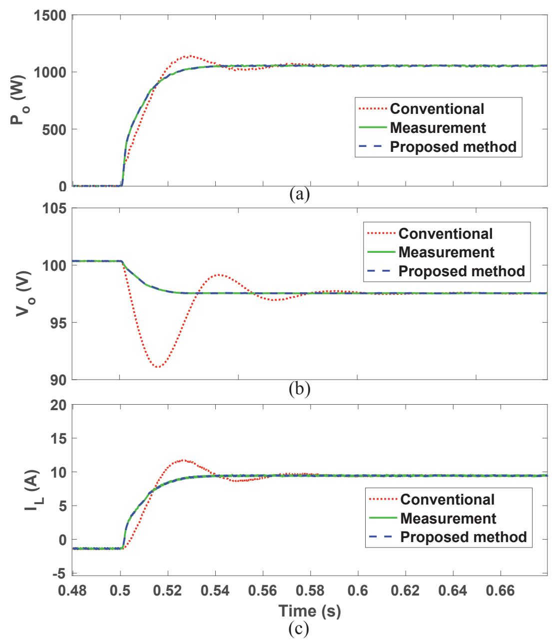

Fig. 5. Simulation performance when the CPL is 1 kW. (a) Load power [W]; Output current [A]; (c) Output voltage [V]; (d) Filter current [A].

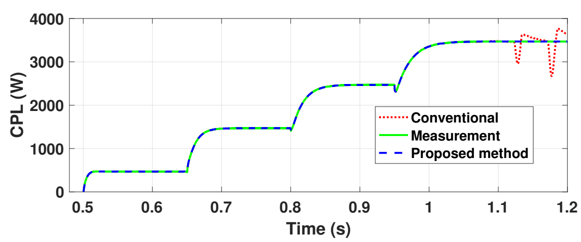

Fig. 6. Step change in CPL.

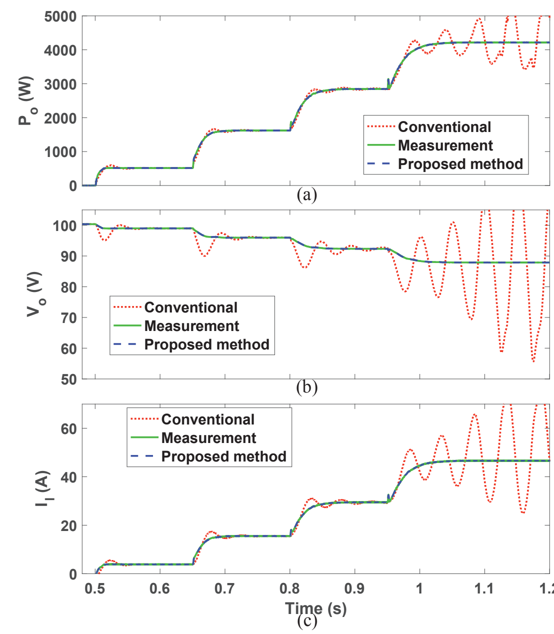

Fig. 7. Simulation performance when the CPL is step changed. (a) Load power [W]; (b) Output voltage [V]; (c) Filter current [A].

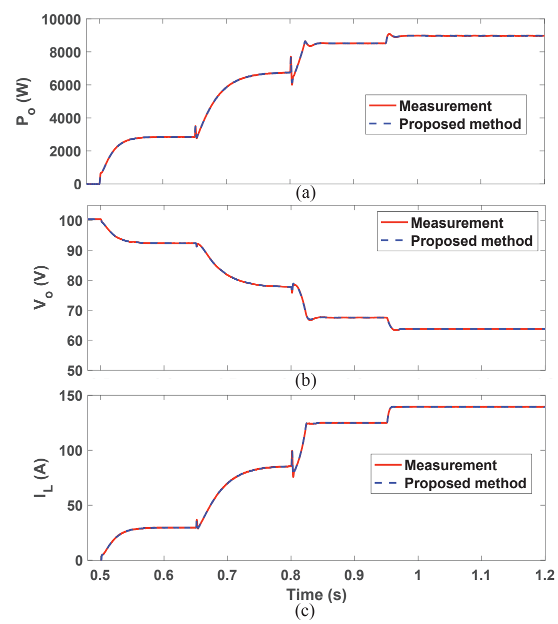

Fig. 8. Simulation performance with larger CPL. (a) Load power [W]; (b) Output voltage [V]; (c) Filter current [A].

measurement sensor, and the proposed current modulation method with the DOB, respectively. At 0.5 s, a CPL of 0.5 kW is connected to the microgrid, and the DC-DC converter decreases its output voltage based on the droop, as shown in Fig. 5(b). As shown in Fig. 5, the proposed method has a smaller overshoot and faster settling time both in the output voltage and current than those obtained using the conventional V-I droop-based dual-loop controller.

B. Step Change of CPLs

In addition, we increase the CPL to 3.5 kW shown in Fig. 6, where the system with the conventional controller becomes unstable, as shown in Fig. 7. However, the proposed method with measurement or DOB can stabilize the system and have a good tracking performance. Moreover, the proposed method with measurement or DOB stabilizes the system even when a larger CPL is connected as shown in Fig. 8. Consequently, we can conclude that the proposed method enlarges the stability region and overcomes the CPL problem.

C. Robustness

In this case study, it is assumed that there exists a parameter mismatch in regards to the capacitor C_f in (15) when the DOB is implemented. The control performance is compared to the presence of C_f variation. which is assumed that it has $\pm 50\%$ error compared with the original value. From Fig. 9, it can be seen that the performance of the output voltage and current is similar to that without C_f variation. It can be concluded that the proposed method is robust to the parameter mismatch.

D. Multi Converters

The proposed method is also tested in the case study where there are four distributed generation (DG) units to support the load in the DC microgrid [37]. Please notice that the line

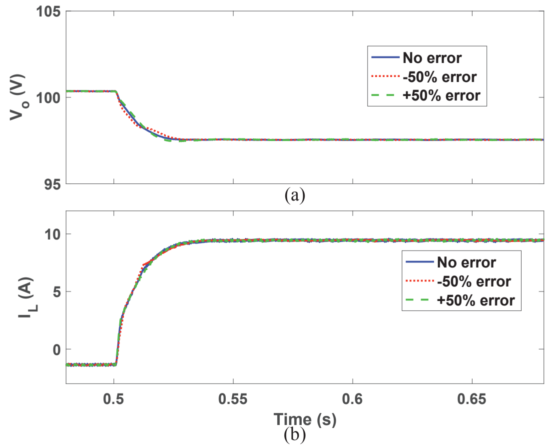

Fig. 9. Robustness performance when the CPL is step changed. (a) Output voltage [V]; (b) Filter current [A].

impedances of converter 1 (DG1) and 3 (DG3) are same. At the first case, all the DGs used the conventional V-I droop-based dual-loop controller, where the control parameters of DG1 and DG4 are the same but different with DG2 and DG3. DG3 has a highest bandwidth and DG2 has a lowest bandwidth. The droop gains were same for all DGs. At the second case, the proposed method is applied to DG1 and DG4. From the results as shown in Fig. 10, it can be seen that the DG1 and DG4 have smaller overshoot and faster convergence time than the first case. The same results are obtained as described in Fig. 7. It should be noted that the current sharing problem is out of this paper and further researched in the future.

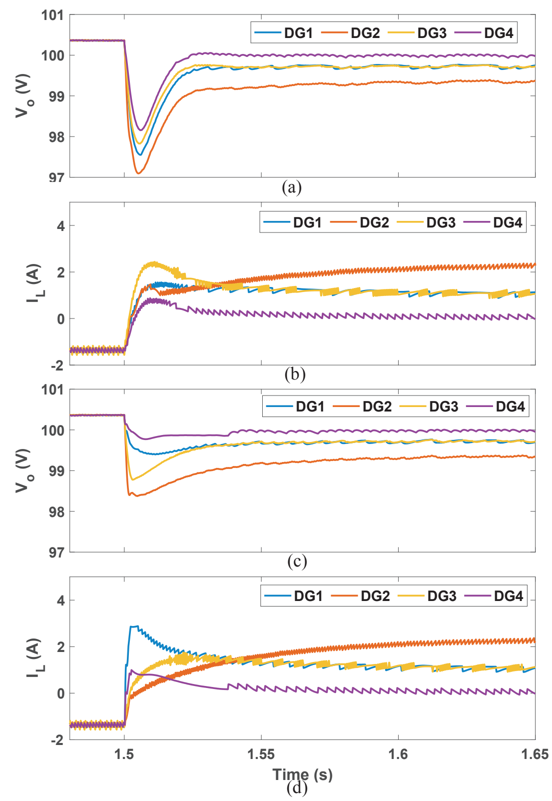

Fig. 10. Conventional V-I droop-based dual-loop controller: (a) output voltage, (b) current; Proposed method in DG1 and DG4 (c) output voltage, (d) current.

V. Experimental Verification

A. Experimental Setup

To verify the effectiveness and stability of the presented control method, experimental setup was established, as shown in Fig. 11(a), by using dSPACE 1006 as the control unit and two Danfoss converters to emulate the DC-DC converter and one converter load, respectively. The CPL is emulated by using a DC electronic load from Chroma. The DC source is provided by a Regatron programable DC power supply. The control desk is used to establish the control interface, which is responsible for controlling the converters and the relays. The experimental results were captured by using the oscilloscope. The configuration of the setup is shown as Fig. 11(b). The converter load and the CPL were connected in parallel, an LC filter was connected between the loads and the DC-DC converter. In the experiments, the sampling and switching frequency were selected as 10kHz. The detailed parameters used in the experiment were the same as those used in the simulations. The experimental results are presented in the following.

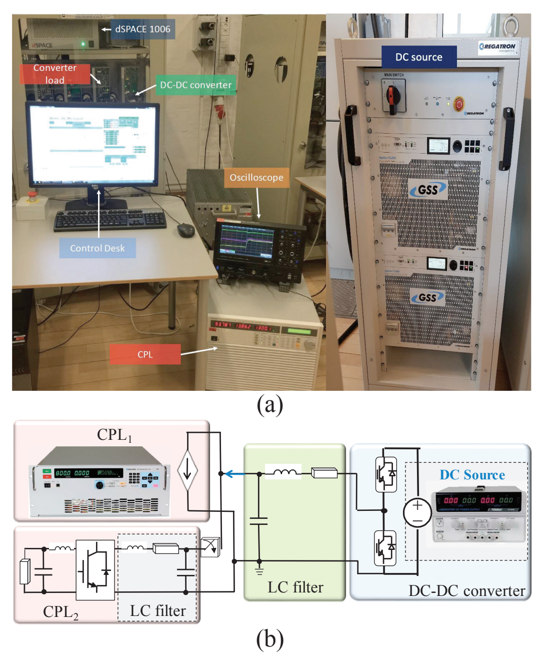

Fig. 11. (a) Experimental setup in the laboratory and (b) electrical scheme.

B. Experimental Results

For the first test, the time response of the PI method, proposed method with the measurement, and proposed method

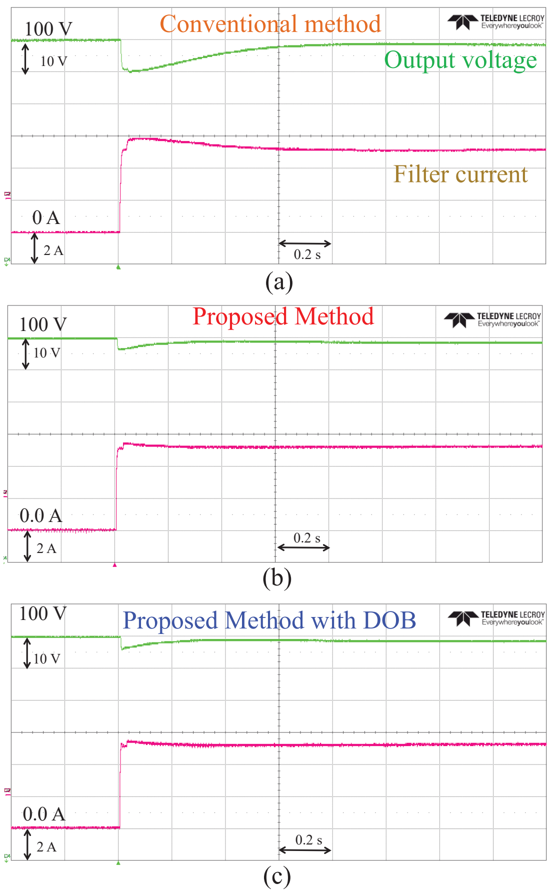

Fig. 12. Measured performance when the CPL is 0.5 kW, using (a) conventional method, (b) proposed method with measurement, (c) with DOB.

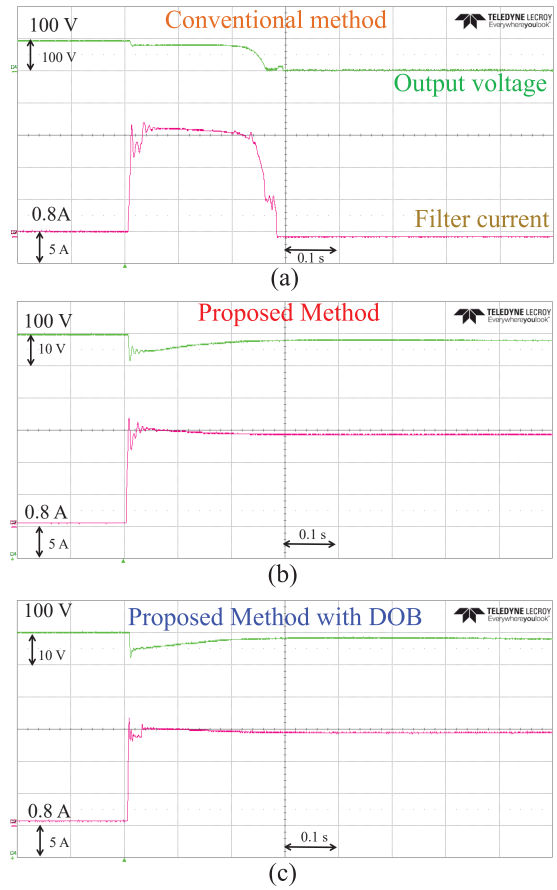

Fig. 13. Measured performance when the CPL is 1.3 kW (full load) using (a) conventional method, (b) proposed method with measurement, (c) proposed method with DOB.

with DOB technique are shown in Fig. 12. All three methods use the same droop coefficient and dual-loop controller gain. It is observed that the output voltage obtained using the proposed method with the measuremen has the smallest overshoot and fastest convergence time as compared to those obtained using other methods. Moreover, the proposed method that uses a DOB produces a close result to the one obtained by the proposed method that uses a current sensor. The three methods for the overshoot and settling time of the output voltage as summarized in Table III. Moreover, we test the case wherein a disturbance is generated by connecting a 1.3 kW CPL, as shown in Fig. 13 At this operating point, we can observe that the system using the conventional method becomes unstable and finally trips down because of the protection system, as shown in Fig. 13(a). However, Figs. 13(b) and 13(c) show a better performance with the proposed methods. Further, we test a disturbance generated by connecting a converter in the DC-link. In this case, the $\text{CPL}_1 = 0.5$ kW is connected first, where the output voltage is initially regulated at 98 V, as shown in Fig. 14. Further, a converter load (CPL_2) suddenly absorbs 0.5 kW more from the DC grid. The proposed methods; (with measurement and DOB) improve the system performance, as shown in Fig. 14. Consequently, it can be concluded that the proposed method is robust to the converter load as well.

TABLE III
COMPARISON OF THE OUTPUT VOLTAGE PERFORMANCE.

Method	Overshoot	Settling time
Conventional method	5.5 V	1 s
Proposed method	1.3 V	0.04 s
Proposed method with DOB	1.5 V	0.05 s

VI. DISCUSSION

The presented results indicate that the proposed method cannot only improve the transient response but also stabilize the DC-DC converter when there exist CPLs in the DC microgrid. The simulation and experimental results matched the theoretical analysis introduced in Section III. It should be noted that the proposed technique with the measurement can be easily plugged into a pre-defined V-I droop-based dual-loop controller with the additional sensor (i.e., output current measurement). In order to remove that sensor, we applied the DOB to the proposed technique, as shown in Fig. 4 which can be easily implemented in the digital controller as well. Finally, the exponential stability of the closed-loop system was guaranteed by the proposed method under the constant power loads and was mathematically proven in a large-signal manner by using the singular perturbation theory. Consequently, the enlarge stability region and robust property can be expected, which are shown in Figs. 6-8.

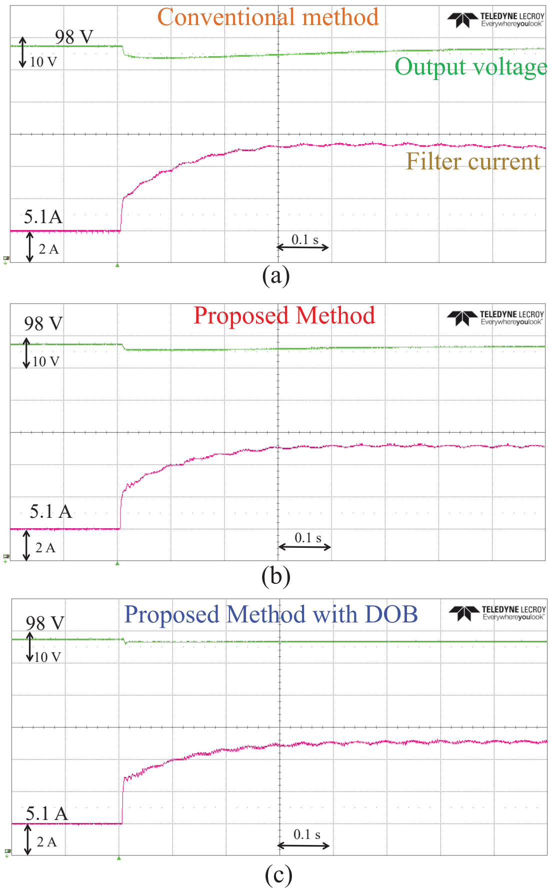

Fig. 14. Measured performance when the converter load is 0.5 kW using (a) conventional method, (b) proposed method with measurement, (c) proposed method with DOB.

In the future work, the stability analysis of the DC microgrid from the system level could be further analyzed when the DC-DC converters use the proposed technique. In addition more advanced controller could be designed based on the proposed technique in order to improve or resolve a certain practical problem.

VII. Conclusions

In this study, we proposed a modified dual-loop controller for DC-DC converters to solve the CPL problems in DC microgrids. The CPL problems can be effectively solved with the addition of an output sensor. Furthermore, to remove the additional sensor, we proposed the use of a DOB to estimate the output current. The V-I droop-based dual-loop controller using feedforward terms was designed to compensate for the output current in the DC-DC converter. For the stability analysis of the system using the proposed method, we used a singular perturbation model to obtain a reduced-order system, and it was verified that the closed-loop system with the proposed method is exponentially stable. Both the simulation and experimental results showed an improvement in the transient response with the usage of proposed method. Moreover, the conventional V-I droop-based dual-loop controller becomes unstable when the CPL is increased, whereas the proposed method stabilizes the system because the output current was rejected by the proposed method.

References

[1] Y. Gui, X. Wang, F. Blaabjerg, and D. Pan, "Control of grid-connected voltage-source converters: The relationship between direct-power control and vector-current control," *IEEE Ind. Electron. Mag.*, vol. 13, no. 2, pp. 31–40, June 2019.

[2] R. Wang, Q. Sun, P. Zhang, Y. Gui, D. Qin, and P. Wang, "Reduced-order transfer function model of the droop-controlled inverter via Jordan continued-fraction expansion," *IEEE Trans. Energy Convers.*, vol. 35, no. 3, pp. 1585–1595, 2020.

[3] S. Gao, H. Zhao, Y. Gui, J. Luo, and F. Blaabjerg, "Impedance analysis of voltage source converter using direct power control," *IEEE Trans. Energy Convers.*, pp. 1–1, 2020.

[4] N. Hatziargyriou, H. Asano, R. Iravani, and C. Marnay, "Microgrids," *IEEE Power Energy Mag.*, vol. 5, no. 4, pp. 78–94, 2007.

[5] T. Dragičević, X. Lu, J. C. Vasquez, and J. M. Guerrero, "DC microgrids—Part I: A review of control strategies and stabilization techniques," *IEEE Trans. Power Electron.*, vol. 31, no. 7, pp. 4876–4891, 2016.

[6] A. Emadi, A. Khaligh, C. H. Rivetta, and G. A. Williamson, "Constant power loads and negative impedance instability in automotive systems: Definition, modeling, stability, and control of power electronic converters and motor drives," *IEEE Trans. Veh. Technol.*, vol. 55, no. 4, pp. 1112–1125, Jul. 2006.

[7] J. Liu, W. Zhang, and G. Rizzoni, "Robust stability analysis of DC microgrids with constant power loads," *IEEE Trans. Power Syst.*, vol. 33, no. 1, pp. 851–860, 2018.

[8] J. Liu, X. Lu, and J. Wang, "Resilience analysis of dc microgrids under denial of service threats," *IEEE Trans. Power Syst.*, vol. 34, no. 4, pp. 3199–3208, 2019.

[9] D. Marx, P. Magne, B. Nahid-Mobarakeh, S. Pierfederici, and B. Davat, "Large signal stability analysis tools in DC power systems with constant power loads and variable power loads—A review," *IEEE Trans. Power Electron.*, vol. 27, no. 4, pp. 1773–1787, 2012.

[10] L. Herrera, W. Zhang, and J. Wang, "Stability analysis and controller design of DC microgrids with constant power loads," *IEEE Transactions on Smart Grid*, vol. 8, no. 2, pp. 881–888, 2017.

[11] R. Han, L. Meng, and J. M. Guerrero, "Hybrid droop control strategy applied to grid-supporting converters in DC microgrids: Modeling, design and analysis," in *43rd Annu. Conf. IEEE Ind. Electron.Soc.*, Oct 2017, pp. 268–273.

[12] A. P. N. Tahim, D. J. Pagano, E. Lenz, and V. Stramosk, "Modeling and stability analysis of islanded DC microgrids under droop control," *IEEE Trans. Power Electron.*, vol. 30, no. 8, pp. 4597–4607, 2015.

[13] M. Su, Z. Liu, Y. Sun, H. Han, and X. Hou, "Stability analysis and stabilization methods of DC microgrid with multiple parallel-connected DC–DC converters loaded by CPLs," *IEEE Trans. Smart Grid*, vol. 9, no. 1, pp. 132–142, 2018.

[14] S. Anand and B. Fernandes, "Reduced-order model and stability analysis of low-voltage DC microgrid," *IEEE Trans. Ind. Electron.*, vol. 60, no. 11, pp. 5040–5049, 2013.

[15] Z. Liu, M. Su, Y. Sun, W. Yuan, H. Han, and J. Feng, "Existence and stability of equilibrium of DC microgrid with constant power loads," *IEEE Trans. Power Syst.*, vol. 33, no. 6, pp. 6999–7010, 2018.

[16] W. Xie, M. Han, W. Cao, J. M. Guerrero, and J. C. Vasquez, "System-level large-signal stability analysis of droop-controlled dc microgrids," *IEEE Trans. Power Electron.*, vol. 36, no. 4, pp. 4224–4236, 2021.

[17] Q. Xu, N. Vafamand, L. Chen, T. Dragičević, L. Xie, and F. Blaabjerg, "Review on advanced control technologies for bidirectional DC/DC converters in DC microgrids," *IEEE J. Emerg. Sel. Topics Power Electron.*, pp. 1–1, 2020.

[18] X. Liu, A. J. Forsyth, and A. M. Cross, "Negative input-resistance compensator for a constant power load," *IEEE Trans. Ind. Electron.*, vol. 54, no. 6, pp. 3188–3196, 2007.

[19] S. R. Huddy and J. D. Skufca, "Amplitude death solutions for stabilization of DC microgrids with instantaneous constant-power loads," *IEEE Trans. Power Electron.*, vol. 28, no. 1, pp. 247–253, 2013.

[20] D. Majstorovic, I. Celanovic, N. D. Teslic, N. Celanovic, and V. A. Katic, "Ultralow-latency hardware-in-the-loop platform for rapid validation of power electronics designs," *IEEE Trans. Ind. Electron.*, vol. 58, no. 10, pp. 4708–4716, 2011.

[21] M. Cespedes, L. Xing, and J. Sun, "Constant-power load system stabilization by passive damping," *IEEE Trans. Power Electron.*, vol. 26, no. 7, pp. 1832–1836, 2011.
[22] A. M. Rahimi and A. Emadi, "Active damping in DC/DC power electronic converters: A novel method to overcome the problems of constant power loads," *IEEE Trans. Ind. Electron.*, vol. 56, no. 5, pp. 1428–1439, 2009.
[23] P. Magne, D. Marx, B. Nahid-Mobarakeh, and S. Pierfederici, "Large-signal stabilization of a dc-link supplying a constant power load using a virtual capacitor: Impact on the domain of attraction," *IEEE Trans. Ind. Appl.*, vol. 48, no. 3, pp. 878–887, 2012.
[24] X. Zhang, X. Ruan, and Q.-C. Zhong, "Improving the stability of cascaded DC/DC converter systems via shaping the input impedance of the load converter with a parallel or series virtual impedance," *IEEE Trans. Ind. Electron.*, vol. 62, no. 12, pp. 7499–7512, 2015.
[25] M. Wu and D. D.-C. Lu, "A novel stabilization method of LC input filter with constant power loads without load performance compromise in DC microgrids," *IEEE Trans. Ind. Electron.*, vol. 62, no. 7, pp. 4552–4562, 2015.
[26] X. Zhu, F. Meng, Z. Xie, and Y. Yue, "An inertia and damping control method of DC–DC converter in DC microgrids," *IEEE Trans. Energy Convers.*, vol. 35, no. 2, pp. 799–807, 2020.
[27] Q. Xu, C. Zhang, C. Wen, and P. Wang, "A novel composite nonlinear controller for stabilization of constant power load in DC microgrid," *IEEE Trans. Smart Grid*, vol. 10, no. 1, pp. 752–761, Jan 2019.
[28] X. Li *et al.*, "Observer-based DC voltage droop and current feed-forward control of a DC microgrid," *IEEE Trans. Smart Grid*, vol. 9, no. 5, pp. 5207–5216, 2018.
[29] J. Neely, S. Pekarek, R. DeCarlo, and N. Vaks, "Real-time hybrid model predictive control of a boost converter with constant power load," in *Proc. 25th Annu. IEEE Appl. Power Electron. Conf. Expo.*, 2010, pp. 480–490.
[30] J. A. Solsona, S. G. Jorge, and C. A. Busada, "Nonlinear control of a buck converter which feeds a constant power load," *IEEE Trans. Power Electron.*, vol. 30, no. 12, pp. 7193–7201, 2015.
[31] Y. Zhao, W. Qiao, and D. Ha, "A sliding-mode duty-ratio controller for DC/DC buck converters with constant power loads," *IEEE Trans. Ind. Appl.*, vol. 50, no. 2, pp. 1448–1458, March 2014.
[32] S. Ding, W. X. Zheng, J. Sun, and J. Wang, "Second-order sliding-mode controller design and its implementation for buck converters," *IEEE Trans. Ind. Inform.*, vol. 14, no. 5, pp. 1990–2000, 2018.
[33] J. Zeng, Z. Zhang, and W. Qiao, "An interconnection and damping assignment passivity-based controller for a DC–DC boost converter with a constant power load," *IEEE Trans. Ind. Appl.*, vol. 50, no. 4, pp. 2314–2322, 2014.
[34] W.-H. Chen, J. Yang, L. Guo, and S. Li, "Disturbance-observer-based control and related methods—An overview," *IEEE Trans. Ind. Electron.*, vol. 63, no. 2, pp. 1083–1095, 2016.
[35] C. Zhang, J. Wang, S. Li, B. Wu, and C. Qian, "Robust control for PWM-based DC–DC buck power converters with uncertainty via sampled-data output feedback," *IEEE Trans. Power Electron.*, vol. 30, no. 1, pp. 504–515, 2015.
[36] Q. Xu, W. Jiang, F. Blaabjerg, C. Zhang, X. Zhang, and T. Fernando, "Backstepping control for large signal stability of high boost ratio interleaved converter interfaced DC microgrids with constant power loads," *IEEE Trans. Power Electron.*, vol. 35, no. 5, pp. 5397–5407, May 2020.
[37] C. Wang, X. Li, L. Guo, and Y. W. Li, "A nonlinear-disturbance-observer-based DC-bus voltage control for a hybrid AC/DC microgrid," *IEEE Trans. Power Electron.*, vol. 29, no. 11, pp. 6162–6177, 2014.
[38] Q. Xu, Y. Xu, C. Zhang, and P. Wang, "A robust droop-based autonomous controller for decentralized power sharing in DC microgrid considering large-signal stability," *IEEE Trans. Ind. Inform.*, vol. 16, no. 3, pp. 1483–1494, 2020.
[39] J. M. Guerrero, J. C. Vasquez, J. Matas, L. G. De Vicuña, and M. Castilla, "Hierarchical control of droop-controlled ac and dc microgrids—a general approach toward standardization," *IEEE Trans. Ind. Electron.*, vol. 58, no. 1, pp. 158–172, 2011.
[40] R. Han, M. Tucci, A. Martinelli, J. M. Guerrero, and G. Ferrari-Trecate, "Stability analysis of primary plug-and-play and secondary leader-based controllers for DC microgrid clusters," *IEEE Trans. Power Syst.*, vol. 34, no. 3, pp. 1780–1800, May 2019.
[41] Y. Gui, F. Blaabjerg, X. Wang, J. Bendtsen, D. Yang, and J. Stoustrup, "Improved DC-link voltage regulation strategy for grid-connected converters," *IEEE Trans. Ind. Electron.*, pp. 1–1, 2020. doi: 10.1109/TIE.2020.2989720.
[42] P. Kokotovic, H. Khalil, and J. O'Reilly, *Singular Perturbation Methods in Control: Analysis and Design*, republished by siam, 1991 ed. Academic Press, New York, 1986.
[43] H. Khalil, *Nonlinear Systems*, 3^{rd} ed. Prentice Hall, 2002.
[44] E. D. Sontag and Y. Wang, "On characterizations of the input-to-state stability property," *Syst. Control Lett,*, vol. 24, no. 5, pp. 351–359, 1995.
[45] ——, "New characterizations of input-to-state stability," *IEEE Trans. Autom. Control*, vol. 41, no. 9, pp. 1283–1294, 1996.

Yonghao Gui (S'11–M'17–SM'20) received the B.S. degree in automation from Northeastern University, Shenyang, China, in 2009, and the M.S. and Ph.D. degrees in electrical engineering from Hanyang University, Seoul, South Korea, in 2012 and 2017, respectively.

From Feb. 2017 to Nov. 2018, he worked with the Department of Energy Technology, Aalborg University, Aalborg, Denmark, as a Postdoctoral Researcher. Since Dec. 2018, he has been working with the Automation & Control Section, Department of Electronic Systems, Aalborg University, Aalborg, Denmark, where he is currently an Assistant Professor. His research interests include Control of Power Electronics in Power Systems and Digitalized Power System.

Dr. Gui has served as an Associate Editor for the IEEE ACCESS and the International Journal of Control, Automation and Systems (IJCAS). He was a recipient of the IEEE Power & Energy Society General Meeting Best Conference Paper Award in 2019 and the IJCAS Academic Activity Award 2019.

Renke Han (S'16-M'18) received the B.S. degree in Automation, the M.S. degree in Control Theory and Control Engineering both from Northeastern University, Liaoning, China, in 2013 and 2015 respectively. He received the Ph.D. degree in Power Electronics Systems from Aalborg University, Aalborg, Denmark, in 2018.

From February 2017 to September 2017, he was as a Visiting Scholar with Laboratoire d'Automatique, École Polytechnique Fédérale de Lausanne (EPFL), Lausanne, Switzerland. Since November 2018, he has been with Power Electronics Group, University of Oxford, UK, as a postdoctoral researcher. His research interests include power electronics converter design including PCB design for power and control circuitries and magnetic elements design, embedded system development, modeling, control and stability analysis for Microgrid.

He was selected as one of six research representatives by University of Oxford, attending Global Young Scientist Summit (GYSS) 2021. He received an outstanding presentation award in Annual Conference of the IEEE Industrial Electronics Society, Italy in 2016 and the Outstanding Master Degree Thesis Award from Liaoning Province, China, in 2014.

Josep M. Guerrero (S'01-M'04-SM'08-FM'15) received the B.S. degree in telecommunications engineering, the M.S. degree in electronics engineering, and the Ph.D. degree in power electronics from the Technical University of Catalonia, Barcelona, in 1997, 2000 and 2003, respectively. Since 2011, he has been a Full Professor with the Department of Energy Technology, Aalborg University, Denmark, where he is responsible for the Microgrid Research Program. From 2014 he is chair Professor in Shandong University; from 2015 he is a distinguished guest Professor in Hunan University; and from 2016 he is a visiting professor fellow at Aston University, UK, and a guest Professor at the Nanjing University of Posts and Telecommunications. From 2019, he became a Villum Investigator by The Villum Fonden, which supports the Center for Research on Microgrids (CROM) at Aalborg University, being Prof. Guerrero the founder and Director of the same centre (www.crom.et.aau.dk).

His research interests is oriented to different microgrid aspects, including power electronics, distributed energy-storage systems, hierarchical and cooperative control, energy management systems, smart metering and the internet of things for AC/DC microgrid clusters and islanded minigrids. Specially focused on microgrid technologies applied to offshore wind, maritime microgrids for electrical ships, vessels, ferries and seaports, and space microgrids applied to nanosatellites and spacecrafts. Prof. Guerrero is an Associate Editor for a number of IEEE TRANSACTIONS. He has published more than 600 journal papers in the fields of microgrids and renewable energy systems, which are cited more than 60,000 times. He received the best paper award of the IEEE Transactions on Energy Conversion for the period 2014-2015, and the best paper prize of IEEE-PES in 2015. As well, he received the best paper award of the Journal of Power Electronics in 2016. During seven consecutive years, from 2014 to 2020, he was awarded by Clarivate Analytics (former Thomson Reuters) as Highly Cited Researcher with 50 highly cited papers. In 2015 he was elevated as IEEE Fellow for his contributions on "distributed power systems and microgrids."

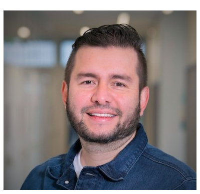

Juan C. Vasquez (M'12-SM'14) received the B.S. degree in electronics engineering from the Autonomous University of Manizales, Manizales, Colombia, and the Ph.D. degree in automatic control, robotics, and computer vision from BarcelonaTech-UPC, Spain, in 2004 and 2009, respectively. He was with the Autonomous University of Manizales working as a teaching assistant and the Technical University of Catalonia as a Post-Doctoral Assistant in 2005 and 2008. In 2011, He was Assistant Professor and in 2014 He was an Associate Professor at the Department of Energy Technology, Aalborg University, Denmark. In 2019, He became a Full Professor and currently He is the Vice Programme Leader of the Microgrids Research Program and codirector of the Center for Reseearch on Microgrids (see crom.et.aau.dk). He was a Visiting Scholar at the Center of Power Electronics Systems (CPES) at Virginia Tech and a visiting professor at Ritsumeikan University, Japan. His current research interests include operation, advanced hierarchical and cooperative control, optimization and energy management applied to distributed generation in AC/DC Microgrids, maritime microgrids, advanced metering infrastructures and the integration of Internet of Things and Energy Internet into the SmartGrid. Prof. Vasquez is a Associate Editor of IET POWER ELECTRONICS the IEEE System Journal and a Guest Editor of a Special Issue in the IEEE TRANSACTIONS ON INDUSTRIAL INFORMATICS on Energy Internet.

Since 2017 Prof. Vasquez was awarded as Highly Cited Researcher by Thomson Reuters and He was the recipient of the Young Investigator Award 2019. He has published more than 500 journal papers in the field of Microgrids, which in total are cited more than 23000 times. Prof. Vasquez is currently a member of the IEC System Evaluation Group SEG4 on LVDC Distribution and Safety for use in Developed and Developing Economies, the Renewable Energy Systems Technical Committee TC-RES in IEEE Industrial Electronics, PELS, IAS, and PES Societies.

Baoze Wei (IEEE Member) received the B.S. degree in electrical engineering, the M.S. degree in power electronics and power drives from Yanshan University, Qinhuangdao, China, and the Ph.D. degree in power electronic systems from the Department of Energy Technology, Aalborg University, Aalborg, Denmark, in 2010, 2014, and 2017, respectively. He is currently working with the Department of Energy Technology, Aalborg University as an assistant professor.

His research interests include AC, DC microgrids, microgrid clusters, modular power inverters for uninterruptible power system, photovoltaic generation system, paralleling power converter for renewable generation systems, power quality, as well as the applications of distributed control.

Wonhee Kim (S'09-M'12) received the B.S. and M.S. degrees in electrical and computer engineering and the Ph.D. degree in electrical engineering from Hanyang University, Seoul, South Korea, in 2003, 2005, and 2012, respectively. From 2005 to 2007, he was with Samsung Electronics Company, Suwon, South Korea. In 2012, he was with the Power and Industrial Systems Research and Development Center, Hyosung Corporation, Seoul. In 2013, he was a Post-Doctoral Researcher with the Institute of Nano Science and Technology, Hanyang University, Seoul, and a Visiting Scholar with the Department of Mechanical Engineering, University of California, Berkeley, CA, USA. From 2014 to 2016, he was with the Department of Electrical Engineering, Dong-A University, Busan, South Korea. He is currently an Associate Professor with the School of Energy Systems Engineering, Chung-Ang University, Seoul. His current research interests include nonlinear control and nonlinear observers, as well as their industrial applications. Dr. Kim has served as an Associate Editor for the IEEE/ASME Transactions Mechatronics, the IEEE ACCESS, and the Journal of Electrical Engineering & Technology.